Assessing Precipitation Trends that may inform Aging Dam Overtopping across the USA

Assessing Precipitation Trends that may inform Aging Dam Overtopping across the USA

Jeongwoo Hwang[1,2]* and Upmanu Lall[1]

[1] Department of Earth and Environmental Engineering, Columbia University, New York, NY-10031, USA

[2] Department of Civil, Construction, and Environmental Engineering, North Carolina State University, Raleigh, NC-27606, USA

* Corresponding author: jhwang24@ncsu.edu

Abstract

In many cases, persistent or recurrent synoptic circulation patterns lead to multiple wet days that precede an extreme rainfall event. The joint occurrence of high antecedent rainfall and extreme rainfall defines a compound event that may pose a high risk for overtopping of aging dams. Our novel analysis assesses whether there are significant trends across the conterminous United States (CONUS) in the joint and individual occurrence of extreme daily precipitation and *k*-day antecedent precipitation extremes, for *k*=5 and *k*=30 days. We find significant trends in the mean and variance of annual maximum daily rainfall, and in the *k*-day antecedent precipitation in certain regions of the CONUS. However, their mutual dependence as measured through a copula is invariant with time. The probability of their joint exceedance, i.e., simultaneously experiencing high extremes of daily precipitation and the k-day precipitation total, is also increasing in many places in the CONUS.

Key Points

- Annual maximum daily precipitation (*A*) and the associated antecedent precipitation (*K*) are increasing in many parts of the United States.
- The probability of the joint extremes of *A* and *K* is increasing even more than that of their individual extremes in many parts of the CONUS.
- The projected flood volume and duration pose concerns for overtopping of dams as they are likely to be full when extreme rainfall occurs.

Plain Summary

Extreme precipitation is becoming more intense and frequent due to global warming, but this does not always result in more intense and frequent flooding. In some cases, certain climate patterns can lead to multiple wet days before an extreme rainfall event, which can raise the risk of flooding, and fill up reservoirs. This study examines the trends in extreme daily precipitation events and in total precipitation over the 5 and 30 days preceding each event across the contiguous United States. We found that the average and variance of both annual maximum daily precipitation and its preceding precipitation total have significant trends in certain parts of the country. The probability for these precipitation variables to co-occur at their extreme levels is increasing in many parts of the United States. The mutual dependence between these two precipitation variables is found to be unchanged over time, which may indicate that the influence of large-scale climate dynamics that create these compound events is not changing, while the precipitation variables themselves may be changing in certain regions. Wetter conditions before an extreme rainy day could increase the chance of reservoir being full and the dam failing by overtopping.

1. Introduction:

The United States has experienced an average of 0.8 flooding events per year that caused more than $1 billion in damages since 1980. This led to over $173 billion in cumulative damage (NOAA National Centers for Environmental Information, 2022). In October 2015, an extreme rainfall and flooding event in South Carolina led to the failure of 36 dams. In 2017, a failure of the main and emergency spillways of the United States' tallest dam, Oroville, in California, led to the evacuation of over 200,000 people and repairs cost over $1.2 billion. In 2020, the failure of two Michigan dams led to the destruction of 150 homes and 10,000 people. These are examples of emerging concerns at the intersection of climate change and aging infrastructure. Of the over 90,000 dams in the USA, at least 1,680 are considered high hazard and rated as in unsatisfactory condition (Lieb et al., 2019). Nearly 34-36% of the historical dam failures are attributed to overtopping (Costa, 1985; Foster et al., 2000), and over 190 of the 250 dam failures during 2010-2019 were classified as hydrologic or flooding failures (Association of State Dam Safety Officials, 2020). It is interesting that most of these failures do not seem to correspond to an extreme rainfall event, but to compound extreme rainfall and antecedent rainfall events that led to high water levels in the reservoir prior to the failure event. The failure of a major dam could have a catastrophic impact. This motivates an understanding of the trends associated with such compound events.

Most of the existing dams across the nation were constructed more than 50 years ago, and their design did not account for the nonstationarity of extremes (Lopez-Cantu & Samaras, 2018; Wright et al., 2019). Increased exposure to overtopping from high flood volumes may increase the chance of catastrophic dam failure and result in socio-economic impacts (Ho et al., 2017; Larrauri & Lall, 2020). Exploring the spatial variation of trends in precipitation over different averaging periods that may influence flood volumes and hence overtopping would help prioritize where to focus risk analysis and mitigation of aging dams.

Potential trends in floods have been assessed based on the observed trends in extreme event precipitation (Bates et al., 2008; Seneviratne et al., 2012). However, many catchments in the United States show a weak linkage between extreme event rainfall and streamflow (Mallakpour & Villarini, 2015; Do et al., 2020). Extreme rainfall has been increasing in both intensity and frequency over large parts of the United States (Trenberth, 2011; Villarini et al., 2011; Kunkel et al., 2013; Rahmani & Harrington, 2019), and climate projections expect such an increase to continue with global warming based on the thermodynamic Clausius-Clapeyron relationship (Trenberth, 2011; Papalexiou & Montanari, 2019). However, despite the increasing trend in extreme precipitation events, there has been limited evidence of intensification in flooding events over the United States (Archfield et al., 2016; Hodgkins et al., 2017; Do et al., 2017), suggesting that an extreme rainfall event alone may not be sufficient to account for extreme floods. This is attributable to the significant influences of other interactive factors of flooding, such as the catchment's antecedent soil moisture conditions and hydrological characteristics (Hodgkins et al., 2017; 2019; Tabari 2020). As an example, although the intensity of rainfall during the Oroville spillway failure in 2017 was relatively moderate (Vahedifard et al., 2017), high antecedent precipitation (October – January) saturated the basin and filled the reservoir, promoting a rapid intensification of runoff during the event (White et al., 2019) that led to the use of the spillway to avoid dam overtopping. The Michigan dam failures in 2020 were also marked by high water levels behind the dam prior to the failure.

The antecedent wetness or soil moisture of a catchment often plays a prominent role in triggering floods under extreme rainfall in many cases (Ivancic & Shaw, 2015; Berghuijs et al., 2019; Nanditha & Mishra, 2022, Wasko & Nathan, 2019; Wasko et al., 2021). This suggests that even beyond the concern with dam filling and overtopping, a joint analysis of trends in the extreme daily rainfall and antecedent rainfall over some averaging period is useful. The decorrelation time scale, as well as the residence time of soil moisture, is usually less than 30 days. Consequently, we considered the joint occurrence of annual maximum daily rainfall and total antecedent rainfall over the prior *k* days (*k*=5, 10, 15, 30) as the compound event of interest for the analysis of trends across the country. To our knowledge, this is the first paper to directly take this approach to derive insights into the flood process without an explicit modeling of continental scale hydrology.

Given the risk perspective, we consider trends in the location, scale, and dependence (coupling) parameters of the annual maximum daily rainfall and the *k*-day antecedent rainfall, as well as in the associated univariate and bivariate return periods of extreme events. Results are reported for *k*=5 and 30 days, and for return periods *T*=10 and 100 years. Nonstationary parametric probability distributions and bivariate copula functions are fit to the data at each location with automatic parameter selection to derive the results. We find substantial variation in trends deemed statistically significant across the country, but the resulting trends are still found to be significant from a field significance analysis and are predominantly increasing.

2. Data and Methods:

2.1. Data

The Climate Prediction Center's (CPC) Global Unified Gauge-Based Analysis of Daily Precipitation (CPC-Global) dataset from the National Oceanic and Atmospheric Administration (NOAA) was used. The CPC-Global is generated by interpolating gauge reports from multiple information sources available at CPC, including the Global Telecommunication System (GTS), Cooperative Observer Network (COOP), and other national and international meteorological agencies. It was shown in an earlier study that the optimal interpolation objective analysis technique, which is used to create the CPC-Global dataset, is capable of generating daily precipitation analysis with biases of less than 1% over most parts of the global and land areas (Chen et al., 2008). The quality of the dataset is assured by performing the quality control on the collected gauge reports by comparing them to the historical records and independent information from measurements at nearby stations, concurrent radar/satellite observations, as well as numerical model forecasts, especially focusing on zero and extreme values (Chen & Xie, 2008). Further detailed information regarding the interpolation algorithm and evaluation processes for generating the CPC product are described in Xie et al. (2007), Xie & Shi (2010), and Chen et al. (2008).

The CPC-Global dataset covers the global land on a daily scale at a 0.5° × 0.5° spatial resolution for a period from 1979 to the present. Only using the data that covers the CONUS from 1979 to 2021, we derived the annual maximum daily precipitation event and its *k*-day antecedent precipitation total for each grid and year.

2.2. Methods

2.2.1. Univariate modeling

The Generalized Extreme Value (GEV) distribution is the limiting distribution of the block maxima of a sequence of independent and identically distributed random (i.i.d.) variables based on the extreme value theorem (see for instance Coles, 2001). It has been a popular choice for analyzing block maxima in the hydrometeorological field. Accordingly, we use the GEV distribution to model the annual maximum daily precipitation. For each grid i, let $A_{i,t}$ denote the annual maximum daily precipitation for year t. The probability distribution for $A_{i,t}$ is specified as:

$$A_{i,t} \sim GEV(\mu_{A_i}, \sigma_{A_i}, \gamma_{A_i}) \tag{1}$$

where μ_{A_i}, σ_{A_i}, and γ_{A_i} are the location, scale, and shape parameters of the GEV distribution at grid i, respectively. The cumulative distribution function of GEV for $A_{i,t}$ is given by:

$$F_{A_i}(A_{i,t}) = e^{-\left[1+\gamma_{A_i}\left(\frac{A_{i,t}-\mu_{A_i}}{\sigma_{A_i}}\right)\right]^{-1/\gamma_{A_i}}} \tag{2}$$

Following Katz (2013), nonstationarity of $A_{i,t}$ is modeled through linear trends in the parameters μ_{A_i}, σ_{A_i} while treating γ_{A_i} as time invariant:

$$\mu_{A_i}(t) = \alpha_1 + \beta_1 t$$
$$\sigma_{A_i}(t) = \alpha_2 + \beta_2 t \quad (3)$$

To model the k-day antecedent precipitation, the 2-parameter gamma distribution (G2) is used. The G2 distribution is considered a reasonable choice for daily or weekly precipitation events (Thom, 1951; Buishand, 1978; Geng et al., 1986). Let $K_{i,t}$ denote the total precipitation over k days preceding the date of the annual maximum precipitation in year t for grid i. Then by reparametrizing $1/{\sigma_{K_i}}^2$ and ${\sigma_{K_i}}^2\mu_{K_i}$ into α_{K_i} and β_{K_i}, respectively, following Johnson et al. (1994), $K_{i,t}$ can be described by G2 as:

$$K_{i,t} \sim G2(\alpha_{K_i}, \beta_{K_i}) \quad (4)$$

where α_{K_i} and β_{K_i} indicate the shape and scale parameters of the G2 distribution at grid i, respectively. The cumulative distribution function of G2 for $K_{i,t}$ is given by:

$$F_{K_i}(K_{i,t}) = \frac{1}{\Gamma(\alpha_{A_i})} \gamma\left(\alpha_{A_i}, \frac{K_{i,t}}{\beta_{A_i}}\right) \quad (5)$$

where Γ is the gamma function and γ is the lower incomplete gamma function. We model the nonstationarity of $K_{i,t}$ through the parameters μ_{K_i} and σ_{K_i} by assuming they change linearly over time:

$$\mu_{K_i}(t) = \alpha_3 + \beta_3 t$$
$$\sigma_{K_i}(t) = \alpha_4 + \beta_4 t \quad (6)$$

These specifications allow us to explore univariate trends in the location and scale parameters of the annual maximum precipitation and k-day precedent precipitation totals at each site. For inference on the parameters of the univariate GEV, we use the package *ismev* in *R* that implements the Maximum Likelihood estimators for the parameters as described in Coles (2001). Estimates are provided for each of the parameters, and their standard errors (se) as well. For the analysis, we map all cases where $|\hat{\beta}|/se(\hat{\beta}) > 2$, as an approximate significance test.

We define:

$$u_{i,t} = F_{A_i}\left(A_{i,t} \middle| \mu_{A_i}(t), \sigma_{A_i}(t), \gamma_{A_i}\right), \qquad v_{i,t} = F_{K_i}\left(K_{i,t} \middle| \mu_{K_i}(t), \sigma_{K_i}(t)\right) \tag{7}$$

The impact of the nonstationarity on each of the univariate extremes of A (r_{A_i}) and K (r_{K_i}) is assessed by computing the ratio of the return level at the end of the given period to the return level at the beginning:

$$r_{A_i} = \frac{F_{A_i}^{-1}\left(1 - \frac{1}{T} \middle| \mu_{A_i}(e), \sigma_{A_i}(e), \gamma_{A_i}\right)}{F_{A_i}^{-1}\left(1 - \frac{1}{T} \middle| \mu_{A_i}(b), \sigma_{A_i}(b), \gamma_{A_i}\right)}, \qquad r_{K_i} = \frac{F_{K_i}^{-1}\left(1 - \frac{1}{T} \middle| \mu_{K_i}(e), \sigma_{K_i}(e)\right)}{F_{K_i}^{-1}\left(1 - \frac{1}{T} \middle| \mu_{K_i}(b), \sigma_{K_i}(b)\right)} \tag{8}$$

where *T* refers to the recurrence interval (e.g., *T*=10 or 100 years) and *e* and *b* refer to the end and beginning of period, respectively. Each estimated ratio's statistical significance is tested using bootstrap resampling. We focus on this as our test of significance for nonstationarity in the quantiles, rather than just the trend coefficients. Recall that only linear trends in the location and scale parameters were modeled.

2.2.2. Bivariate modeling

To test whether the dependence between $A_{i,t}$ and $K_{i,t}$ is changing with time, we consider whether the correlation ρ_i between $u_{i,t}$ and $v_{i,t}$ changes with time. Note that by Equation (7), the temporal trends in the mean and variance of $A_{i,t}$ and $K_{i,t}$ are effectively addressed in the construction of $u_{i,t}$ and $v_{i,t}$, and thus we expect the mean and variance of $u_{i,t}$ and $v_{i,t}$ are constant over time. Then an estimate of ρ_i would be provided by:

$$\hat{\rho}_i = \frac{\sum(u_{i,t} - m_{u_i})(v_{i,t} - m_{v_i})}{s_{u_i}s_{v_i}} = \frac{\sum(u_{i,t}v_{i,t} - m_{u_i}v_{i,t} - u_{i,t}m_{v_i})}{s_{u_i}s_{v_i}} = \frac{\sum(u_{i,t}v_{i,t}) - 2m_{u_i}\, m_{v_i}}{s_{u_i}s_{v_i}} \quad (9)$$

where m_{u_i}, m_{v_i}, s_{u_i}, and s_{v_i} are the mean and standard deviation of $u_{i,t}$ and $v_{i,t}$, respectively. If the dependence between $u_{i,t}$ and $v_{i,t}$ is stationary, then the expected value of the cross product $w_{i,t} = u_{i,t}v_{i,t}$ should be invariant with time. We explore the stationarity of $w_{i,t}$ using the Mann-Kendall test, to assess whether modeling the nonstationarity in the dependence structure is needed. We found significant trends in only a few places (less than 1%) in the CONUS. This was not significant based on a field significance test, implying a stationary dependence structure could be considered for bivariate models of $A_{i,y}$ and $K_{i,y}$.

Copulas have been used extensively for modeling the dependence of multivariate random. Since the dependence structure was identified as stationary, the multivariate cumulative distribution function of $A_{i,y}$ and $K_{i,y}$ is represented in terms of their marginal of $u_{i,t}$ and $v_{i,t}$, with a stationary copula function C_i, defined by a copula parameter θ:

$$F_{A_i,K_i}(A_{i,t}, K_{i,t}) = C_i(u_{i,t}, v_{i,t}; \theta) \quad (10)$$

There are several parametric copula families available, and the strength of bivariate dependence is usually controlled by θ. Using the package *VineCopula* in *R* (Nagler et al., 2022), we determine the optimal set of copula family and θ that best fits a given bivariate distribution based on the Bayesian Information Criterion (BIC) statistics for each grid *i*.

Since we consider the nonstationarity of $A_{i,t}$ and $K_{i,t}$, their probability distributions are assumed to vary with time, and thus the probability of their joint exceedances for a fixed set of thresholds is also expected to be time dependent. Here, we measure the probability of joint exceedances for a fixed set of thresholds A_i^* and K_i^* at time *t*, i.e., $p(A_{i,t} > A_i^*,\ K_{i,t} > K_i^*)$, using copulas (Tilloy et al., 2022):

$$p\left(A_{i,t} > A_i^*, K_{i,t} > K_i^*\right) = G_t(A_i^*, K_i^*) = 1 - u_{i,t}^* - v_{i,t}^* + C_i\left(u_{i,t}^*, v_{i,t}^*; \theta\right) \tag{11}$$

$$u_{i,t}^* = F_{A_i}\left(A_i^* \middle| \mu_{A_i}(t), \sigma_{A_i}(t), \gamma_{A_i}\right), \qquad v_{i,t}^* = F_{K_i}\left(K_i^* \middle| \mu_{K_i}(t), \sigma_{K_i}(t)\right) \tag{12}$$

Then we compute the change in the probability of joint exceedances by calculating $G_e(A_i^*, K_i^*)/G_b(A_i^*, K_i^*)$, where *e* and *b* refer to the end and beginning of the period. We present the results for the joint occurrence of an annual maximum daily precipitation event exceeding its 100-year return level following a *k*-day antecedent precipitation total greater than its 10-year return level. Consequently, A_i^* and K_i^* are set as the 100-year return level of $A_{i,t}$ and 10-year return level of $K_{i,t}$, respectively, based on the probability distributions at *t*=*b*. A significance test was performed for the estimated ratios at the 5% level for each grid *i* using bootstrap resampling.

3. Results

3.1 Spatial patterns of univariate trends

During the period of record, the location parameter of *A*, μ_A, has increased significantly over the eastern half of the CONUS while there are mixed trends in the western half (Figure 1a). Broadly speaking, these geographical contrasts are consistent with the findings from earlier studies (Easterling et al., 2017; Wright et al., 2019; Harp & Horton, 2022). The scale parameter of *A*, σ_A, has increased across the CONUS, in multiple spatial clusters partially covering regions in the northwest, southwest, and the east coast (Figure 1b). Areas where both μ_A and σ_A show an increasing trend, such as the northeastern region, would have an amplified increase in the probability of extreme rainfall (Figure S.1a).

However, the location parameter of *K*, μ_K, has decreased throughout the CONUS, except for some regions including the states of Wyoming, Idaho, and Montana, for both cases of *k*=5 and *k*=30 days (Figures 1c and 1e). The scale parameter of *K*, σ_K, shows different patterns for *k*=5 and *k*=30 days. When *k*=5 days, σ_K shows statistically significant increases in the eastern half of the CONUS relative to the west, except in some regions in the northwest and near the states of Colorado and Oregon (Figure 1d). When *k*=30 days, σ_K shows statistically significant increases mostly in the southwestern regions (Figures 1f). For most locations where trends in μ_K and σ_K are both significant, μ_K shows a decreasing trend while σ_K increases, for both cases of *k*=5 and *k*=30 days (Figures S.1b and S.1c). This is interesting since the implications for antecedent precipitation prior to an extreme event are quite mixed. An increase in the variance, but a decrease in the mean value could still portend a higher risk of an extreme event, since it would reflect more frequent smaller and less frequent but potentially larger total precipitation.

Most cases where both μ_A and μ_K increase appear scattered in the western half of the CONUS, especially within the northwestern regions (Figure S.2a). Interestingly, μ_A and μ_K show negative trends in regions near the west coast, and many of these cases are in the vicinity of the regions where both parameters have increased (Figure S.2b). These spatial patterns of simultaneous increases/decreases in μ_A and μ_K represent where the changing climate is likely to further amplify/damp potential flood risk.

Linear trends in the univariate extremes of *A* and *K* were also explored in terms of their 10-year and 100-year return levels. The spatial variability of these trends is shown in Figure 2. The 10-year and 100-year return levels of *A* show similar spatial patterns of significant changes across the CONUS, mostly composed of positive trends (Figure 2a and 2b). It is notable that the northeastern region has significant increases in the 10-year and 100-year return levels of *A*, consistent with the significant increases in the location parameter of *A* observed in Figure 1a.

The 10-year and 100-year return levels of *K* have changed significantly as well across the CONUS, regardless of the *k* value. Their spatial trends are similar to each other, with low spatial coherence – significant positive trends often occur close to significant negative trends. For both cases of *k*=5 and *k*=30 days, many locations have shown significant changes in the 10-year and 100-year return levels of *K* but only a few spatial clusters of them are visually detectable. For k=5 days, the 10-year and 100-year return levels of K have increased the most in the states of Wyoming and Montana, and eastern Texas. At the same time, areas near the state of Oklahoma and northern Texas have experienced a significant decrease in those return levels of K (Figures 2c and 2d). For k=30 days, the 10-year and 100-year return levels of K have increased the most near the states of Montana, Wyoming, and Colorado, and decreased the most in regions including the states of Arizona, Nevada, northern Texas, and the southeastern regions (Figures 2e and 2f). In closing, we remind the reader that the 5- and 30-day precipitation totals (K) analyzed here are conditional on the subsequent occurrence of an annual maximum daily rainfall event (A), and do not refer to the 5- or 30-day annual maximum precipitation.

3.2 Bivariate trend analyses

When k=5 days, a strong dependence between A and K is identified in clusters mainly along the western coast and in some regions near the states of Montana, Wyoming, and Missouri (Figure S.3a). When k=30 days, such a strong dependence is also observed in other regions as well, particularly over the eastern half of the CONUS, including the states of Kansas, Missouri, Iowa, Wisconsin, and the southeastern regions (Figure S.3b). For these locations, A is expected to have greater magnitudes with a wetter precedent 30-day period, K, reflecting a persistent wet weather regime, that would be a concern for flood generation and dam safety.

For both k=5 and k=30 days, in most cases, radially asymmetric copula families, such as Gumbel, Clayton, and Joe copulas, were identified as best explaining the dependence structure between A and K using the BIC criteria (Figures S.4a and S.4b). Based on the fitted copula model, linear trends in the probability of joint exceedances were estimated, and their spatial variability is shown in Figure 3. For k=5 days, there have been significant increases in the joint probability of A exceeding its 100-year event (A_{100}) and K exceeding its 10-year event (K_{10}) across the CONUS, particularly in parts of the states of California, Washington, Idaho, Colorado, Nebraska, Minnesota, and in the northeastern regions (Figure 3a). Similar spatial patterns of such increases are observed for k=30 days as well, but with denser clusters and greater magnitudes (Figure 3b).

4. Summary and Discussion

We motivated the analysis of the joint trends in annual maximum daily rainfall and the antecedent k-day rainfall from the perspective that these two variables jointly determine flood potential. The potential failure of a large number of aging dams in the United States by overtopping under a changing climate is the driving practical concern. To address this, one would need an analysis of the daily inflows into each of the more than 90,000 reservoirs, and information on their flood operating rules, to estimate the flood volume that could lead to overtopping. Such information is not forthcoming. Consequently, using these two rainfall variables as a proxy became necessary. The general framework followed was to consider a nonstationary, probabilistic model of the univariate and joint exceedance probabilities of the annual maximum daily rainfall and the antecedent k-day rainfall across the country. Using this analysis, one could identify regions with increasing trends in the rare events associated with both the annual maximum daily rainfall event and the antecedent rainfall. Where these are statistically significant, there may be increasing concern for the potential overtopping of dams. We developed a model for the purpose, and provide results for selected return periods and durations of antecedent rainfall. The model includes a consideration of the dependence between the annual maximum daily rainfall and the antecedent k-day rainfall. Where this dependence is high, the underlying synoptic meteorology is prone to persistent periods of rainfall that culminate in an extreme rainfall event. This is an area of concern, especially where both types of rainfall have positive trends.

Our analysis of trends in the annual maximum 1-day precipitation (*A*) and the total precipitation for *k* days preceding the annual maximum (*K*) revealed that the average magnitude of *A* has been increasing across the eastern half of the CONUS, while *K* has been decreasing, on average, in most places in the CONUS, except for regions near the states of Wyoming, Idaho, and Montana. These stark differences between the spatial trends in *A* and *K* may partially explain why flood magnitudes have shown unclear trends despite the significant increase in precipitation extremes across the CONUS (Archfield et al., 2016; Slater & Villarini, 2016). Trends in the univariate extremes of *A* and *K* were also explored in terms of the 10-year and 100-year events. The rainfall associated with the 10-year and 100-year return levels of the daily annual maximum has been increasing in general across the CONUS. For the preceding period rainfall, the 10-year and 100-year return levels have increased in many places in the CONUS, but their spatial patterns were more fragmented. The probability of annual maximum daily precipitation event exceeding its 100-year return level following a *k*-day antecedent precipitation total greater than its 10-year return level has been increasing across multiple areas in the CONUS.

The seasonality of precipitation varies across the country, as do the dominant mechanisms of rainfall. Since our focus was a national scale characterization of the changing risk of the joint increase in antecedent and annual maximum daily rainfall, we have not explored the details of the changes in synoptic conditions to see whether the frequency and persistence of the meteorological factors responsible for extreme rainfall have changed. Since the correlation of the *k*-day and the annual maximum day rainfall does not appear to change with time anywhere in the country, one may speculate that the mechanism associated with the wet spells that culminate in the annual maximum daily rainfall event has not changed. However, there are indications that the amount of rain associated with this mechanism has increased for both types of rainfall in many parts of the country. Even where the antecedent *k*-day rainfall has decreased, its variance has increased. As a result, the trends in the magnitude of the *T*-year event (*T*=10 and 100) show an increase in most of these locations. There are many more significant trends in the *k*-day rainfall than in the annual maximum daily rainfall over the past 43 years. This is also interesting since the increased antecedent rainfall would correspond to a higher runoff potential for even a relatively modest rainfall event and lead to reservoir full conditions that would be a concern for dam overtopping. This observation is consistent with the observed recent dam failure events that have typically not been associated with catastrophic daily rainfall.

Acknowledgements

This research is based upon work supported in part by the Institute for Geospatial Understanding through an Integrative Discovery Environment (I-GUIDE) that is funded by the National Science Foundation (NSF) under award No. 2118329. Partial support was also provided by the NSF within the framework of America's Water Risk: Water System Data Pooling for Climate Vulnerability Assessment and Warning System, award No. 2040613. Any opinions, findings, conclusions, or recommendations expressed in this material are those of the author(s) and do not necessarily reflect the views of NSF.

Data Availability

The Climate Prediction Center's (CPC) Global Unified Gauge-Based Analysis of Daily Precipitation (CPC-Global) dataset may be obtained from NOAA PSL, Boulder, Colorado, USA, from their website at <https://psl.noaa.gov/data/gridded/data.cpc.globalprecip.html>.

References

Archfield, S. A., Hirsch, R. M., Viglione, A., & Blöschl, G. (2016). Fragmented patterns of flood change across the United States. *Geophysical Research Letters*, *43*(19), 10-232.

Association of State Dam Safety Officials (2020, August 1). *Dam Incident Database Search*. https://www.damsafety.org/incidents/

Barbero, R., Fowler, H. J., Lenderink, G., & Blenkinsop, S. (2017). Is the intensification of precipitation extremes with global warming better detected at hourly than daily resolutions?. *Geophysical Research Letters*, *44*(2), 974-983.

Bates, B., Kundzewicz, Z., & Wu, S. (2008). *Climate change and water*. Intergovernmental Panel on Climate Change Secretariat.

Berghuijs, W. R., Harrigan, S., Molnar, P., Slater, L. J., & Kirchner, J. W. (2019). The relative importance of different flood-generating mechanisms across Europe. *Water Resources Research*, *55*(6), 4582-4593.

Bouwer, L. M. (2011). Have disaster losses increased due to anthropogenic climate change?. *Bulletin of the American Meteorological Society*, *92*(1), 39-46.

Buishand, T. A. (1978). Some remarks on the use of daily rainfall models. *Journal of Hydrology*, *36*(3-4), 295-308.

Chen, M., & Xie, P. (2008). Quality Control of Daily Precipitation Reports at NOAA/CPC, paper presented at AMS 12th conferences on IOAS-AOLS, 20-24 January New Orleans, LA.

Chen, M., Shi, W., Xie, P., Silva, V. B., Kousky, V. E., Wayne Higgins, R., & Janowiak, J. E. (2008). Assessing objective techniques for gauge-based analyses of global daily precipitation. *Journal of Geophysical Research: Atmospheres*, *113*(D4).

Coles, S. (2001). Classical extreme value theory and models. In *An introduction to statistical modeling of extreme values* (pp. 45-73). Springer, London.

Costa, J. E. (1985). *Floods from dam failures* (Vol. 85, No. 560). US Geological Survey.Do, H. X., Mei, Y., & Gronewold, A. D. (2020). To what extent are changes in flood magnitude related to changes in precipitation extremes?. *Geophysical Research Letters*, *47*(18), e2020GL088684.

Do, H. X., Westra, S., & Leonard, M. (2017). A global-scale investigation of trends in annual maximum streamflow. *Journal of hydrology*, *552*, 28-43.

Easterling, D., Kunkel, K., Arnold, J., Knutson, T., LeGrande, A., Leung, L., ... & Wehner, M. (2017). Precipitation change in the United States. In climate science special report: fourth national climate assessment, volume I. [Wuebbles D, Fahey D, Hibbard K, Dokken D, Stewart B, Maycock T (eds.)]. US Global Change Research Program, Washington, DC, 207–230.

Foster, M., Fell, R., & Spannagle, M. (2000). The statistics of embankment dam failures and accidents. *Canadian Geotechnical Journal*, *37*(5), 1000-1024.Geng, S., de Vries, F. W. P., & Supit, I. (1986). A simple method for generating daily rainfall data. *Agricultural and Forest meteorology*, *36*(4), 363-376.

Groisman, P. Y., Knight, R. W., Easterling, D. R., Karl, T. R., Hegerl, G. C., & Razuvaev, V. N. (2005). Trends in intense precipitation in the climate record. *Journal of climate*, *18*(9), 1326-1350.

Harp, R. D., & Horton, D. E. (2022). Observed Changes in Daily Precipitation Intensity in the United States. *Geophysical Research Letters*, e2022GL099955.

Ho, M., Lall, U., Allaire, M., Devineni, N., Kwon, H. H., Pal, I., ... & Wegner, D. (2017). The future role of dams in the United States of America. *Water Resources Research*, *53*(2), 982-998.

Hodgkins, G. A., Dudley, R. W., Archfield, S. A., & Renard, B. (2019). Effects of climate, regulation, and urbanization on historical flood trends in the United States. *Journal of Hydrology*, *573*, 697-709.

Hodgkins, G. A., Whitfield, P. H., Burn, D. H., Hannaford, J., Renard, B., Stahl, K., ... & Wilson, D. (2017). Climate-driven variability in the occurrence of major floods across North America and Europe. *Journal of Hydrology*, *552*, 704-717.

Ivancic, T. J., & Shaw, S. B. (2015). Examining why trends in very heavy precipitation should not be mistaken for trends in very high river discharge. *Climatic Change*, *133*(4), 681-693.

Johnson, N. L., Kotz, S., & Balakrishnan, N. (1994). *Continuous Univariate Distributions, Volume I, 2nd edn*. Wiley, New York.

Katz, R. W. (2013). Statistical methods for nonstationary extremes. In *Extremes in a changing climate* (pp. 15-37). Springer, Dordrecht.

Kunkel, K. E., Karl, T. R., Brooks, H., Kossin, J., Lawrimore, J. H., Arndt, D., ... & Wuebbles, D. (2013). Monitoring and understanding trends in extreme storms: State of knowledge. *Bulletin of the American Meteorological Society*, *94*(4), 499-514.

Larrauri, P., & Lall, Upmanu. (2020). Assessing the exposure of critical infrastructure and other assets to the climate induced failure of aging dams in the US. *Final Report for the Global Risk Institute*.

Lieb, D. A., Casey, M., & Minkoff, M. (2019, Nov. 11). *At least 1,680 dams across the US pose potential risk*. The Associated Press. https://apnews.com/article/ne-state-wire-us-news-ap-top-news-sc-state-wire-dams-f5f09a300d394900a1a88362238dbf77

Lopez-Cantu, T., & Samaras, C. (2018). Temporal and spatial evaluation of stormwater engineering standards reveals risks and priorities across the United States. *Environmental Research Letters*, *13*(7), 074006.

Mallakpour, I., & Villarini, G. (2015). The changing nature of flooding across the central United States. *Nature Climate Change*, *5*(3), 250-254.

Mallakpour, I., AghaKouchak, A., & Sadegh, M. (2019). Climate-induced changes in the risk of hydrological failure of major dams in California. *Geophysical Research Letters*, *46*(4), 2130-2139.

Nagler, T., Schepsmeier, U., Stoeber, J., Brechmann., E. C., Graeler, B., & Erhardt T. (2022). VineCopula: Statistical Inference of Vine Copulas. *R package version 2.4.4*. https://CRAN.R-project.org/package=VineCopula

Nanditha, J. S., & Mishra, V. (2022). Multiday Precipitation Is a Prominent Driver of Floods in Indian River Basins. *Water Resources Research*, *58*(7), e2022WR032723.

NOAA National Centers for Environmental Information (NCEI) (2022). *U.S. Billion-Dollar Weather and Climate Disasters*. https://www.ncdc.noaa.gov/billions/

Papalexiou, S. M., & Montanari, A. (2019). Global and regional increase of precipitation extremes under global warming. *Water Resources Research*, *55*(6), 4901-4914.

Rahmani, V., & Harrington Jr, J. (2019). Assessment of climate change for extreme precipitation indices: A case study from the central United States. *International Journal of Climatology*, *39*(2), 1013-1025.

Seneviratne, S. I., Nicholls, N., Easterling, D., Goodess, C., Kanae, S., Kossin, J., ... & Zhang, X. (2012). Managing the Risks of Extreme Events and Disasters to Advance Climate Change Adaptation. A Special Report of Working Groups I and II of the Intergovernmental Panel on Climate Change (IPCC).

Slater, L. J., & Villarini, G. (2016). Recent trends in US flood risk. *Geophysical Research Letters*, *43*(24), 12-428.

Stephens, C. M., Johnson, F. M., & Marshall, L. A. (2018). Implications of future climate change for event-based hydrologic models. *Advances in Water Resources*, *119*, 95-110.

Heffernan, J. E., Stephenson, A. G., & Gilleland, E. (2018). ismev: An introduction to statistical modeling of extreme values. *R package version 1.42*. https://CRAN.R-project.org/package=ismev

Thom, H. C. (1951). A frequency distribution for precipitation. *Bulletin of the American Meteorological Society*, *32*(10), 397.

Tilloy, A., Malamud, B. D., Winter, H., & Joly-Laugel, A. (2020). Evaluating the efficacy of bivariate extreme modelling approaches for multi-hazard scenarios. *Natural Hazards and Earth System Sciences*, *20*(8), 2091-2117.

Trenberth, K. E. (2011). Changes in precipitation with climate change. *Climate research*, *47*(1-2), 123-138.

Vahedifard, F., AghaKouchak, A., Ragno, E., Shahrokhabadi, S., & Mallakpour, I. (2017). Lessons from the Oroville dam. *Science*, *355*(6330), 1139-1140.

Villarini, G., Smith, J. A., Baeck, M. L., Vitolo, R., Stephenson, D. B., & Krajewski, W. F. (2011). On the frequency of heavy rainfall for the Midwest of the United States. *Journal of Hydrology*, *400*(1-2), 103-120.

Visser, H., Petersen, A. C., & Ligtvoet, W. (2014). On the relation between weather-related disaster impacts, vulnerability and climate change. *Climatic change*, *125*(3), 461-477.

Wasko, C., & Nathan, R. (2019). Influence of changes in rainfall and soil moisture on trends in flooding. *Journal of Hydrology*, *575*, 432-441.

Wasko, C., Nathan, R., & Peel, M. C. (2020). Changes in antecedent soil moisture modulate flood seasonality in a changing climate. *Water Resources Research*, *56*(3), e2019WR026300.

Wasko, C., Nathan, R., Stein, L., & O'Shea, D. (2021). Evidence of shorter more extreme rainfalls and increased flood variability under climate change. *Journal of Hydrology*, *603*, 126994.

Wentz, F. J., Ricciardulli, L., Hilburn, K., & Mears, C. (2007). How much more rain will global warming bring?. *Science*, *317*(5835), 233-235.

Westra, S., Alexander, L. V., & Zwiers, F. W. (2013). Global increasing trends in annual maximum daily precipitation. *Journal of climate*, *26*(11), 3904-3918.

White, A. B., Moore, B. J., Gottas, D. J., & Neiman, P. J. (2019). Winter storm conditions leading to excessive runoff above California's Oroville Dam during January and February 2017. *Bulletin of the American Meteorological Society*, *100*(1), 55-70.

Wing, O. E., Lehman, W., Bates, P. D., Sampson, C. C., Quinn, N., Smith, A. M., ... & Kousky, C. (2022). Inequitable patterns of US flood risk in the Anthropocene. Nature Climate Change, 12(2), 156-162.

Wright, D. B., Bosma, C. D., & Lopez-Cantu, T. (2019). US hydrologic design standards insufficient due to large increases in frequency of rainfall extremes. *Geophysical Research Letters*, *46*(14), 8144-8153.

Xie, P., Chen, M., & Shi, W. (2010). CPC unified gauge-based analysis of global daily precipitation. In *Preprints, 24th Conf. on Hydrology, Atlanta, GA, Amer. Meteor. Soc* (Vol. 2).

Xie, P., Chen, M., Yang, S., Yatagai, A., Hayasaka, T., Fukushima, Y., & Liu, C. (2007). A gauge-based analysis of daily precipitation over East Asia. *Journal of Hydrometeorology*, *8*(3), 607-626.

Figures

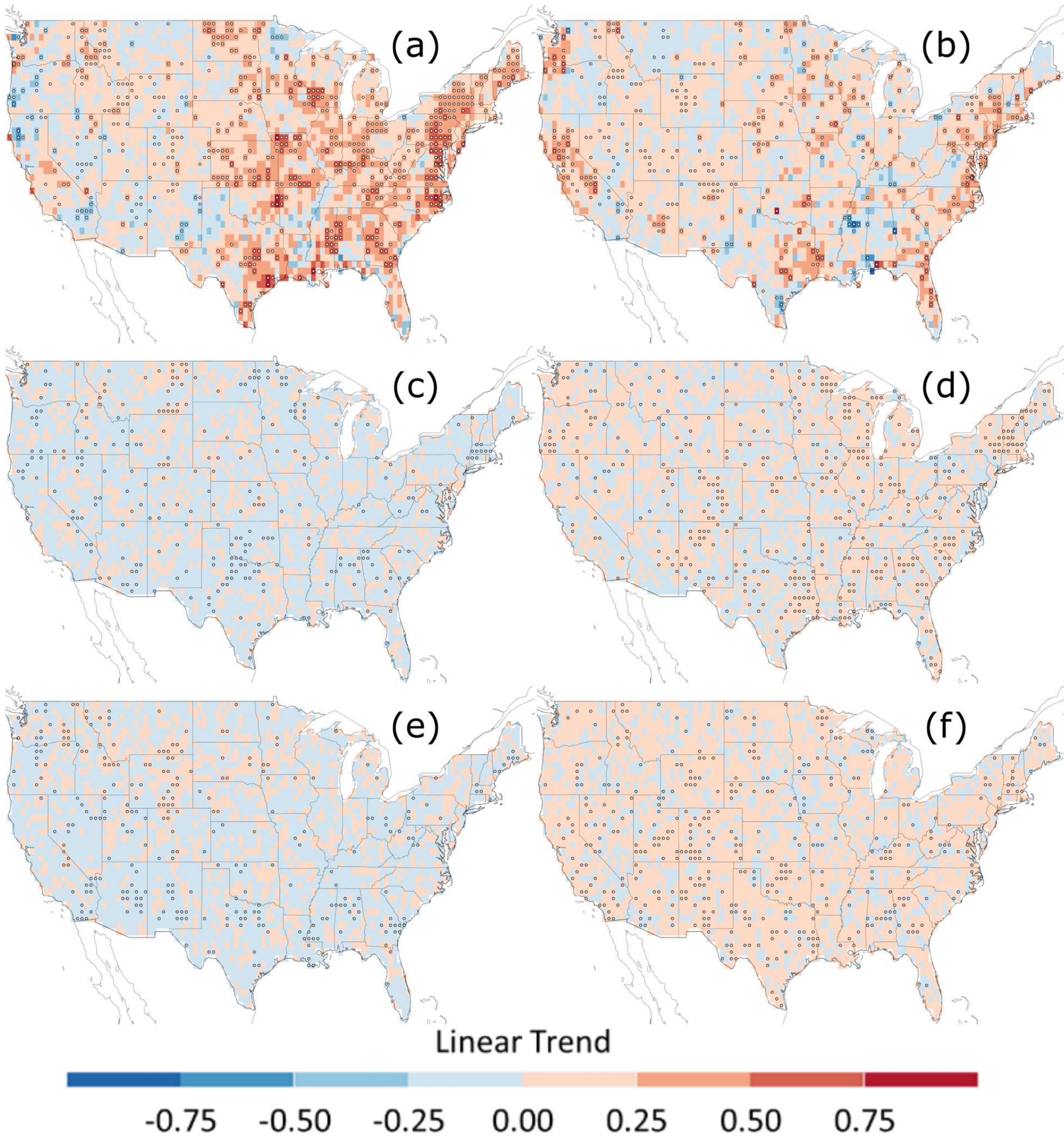

Figure 1. Spatial trends in the (a) location parameter of *A*, (b) scale parameter of *A*, (c) location parameter of 5-day *K*, (d) scale parameter of 5-day *K*, (e) location parameter of 30-day *K*, and (f) scale parameter of 30-day *K*. Statistically significant estimates (p-value < 0.05) are represented with white circles. The colors indicate the linear slope of estimated trends.

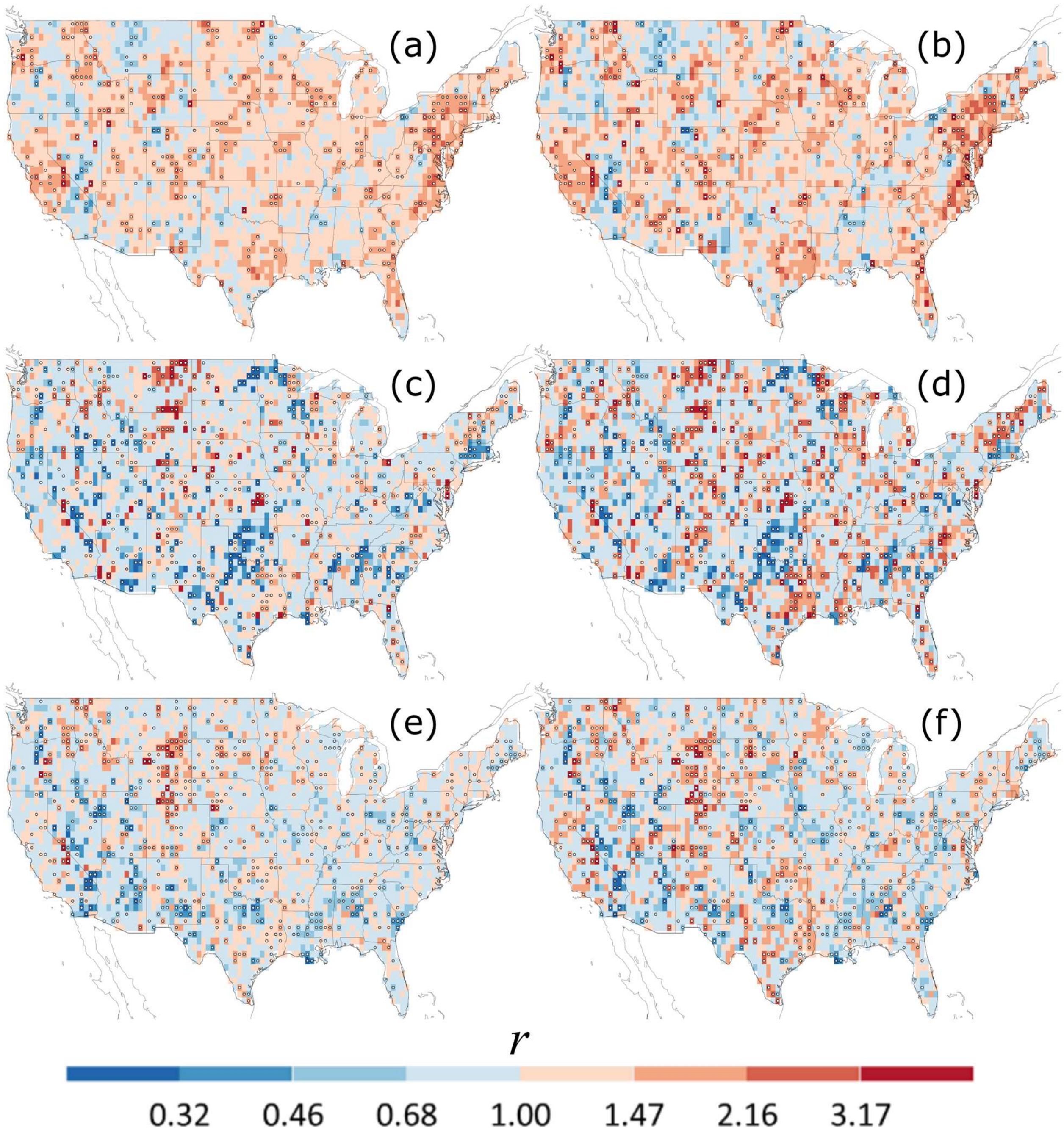

Figure 2. Spatial trends in the 10-year return level of (a) *A*, (c) 5-day *K*, and (e) 30-day *K* and 100-year return level of (b) *A*, (d) 5-day *K*, and (f) 30-day *K*. Statistically significant estimates (p-value < 0.05) are represented with white circles. The color indicates the ratio (r) of the return level at the end of the given period to the return level at the beginning. Details of r are presented in Equation (8).

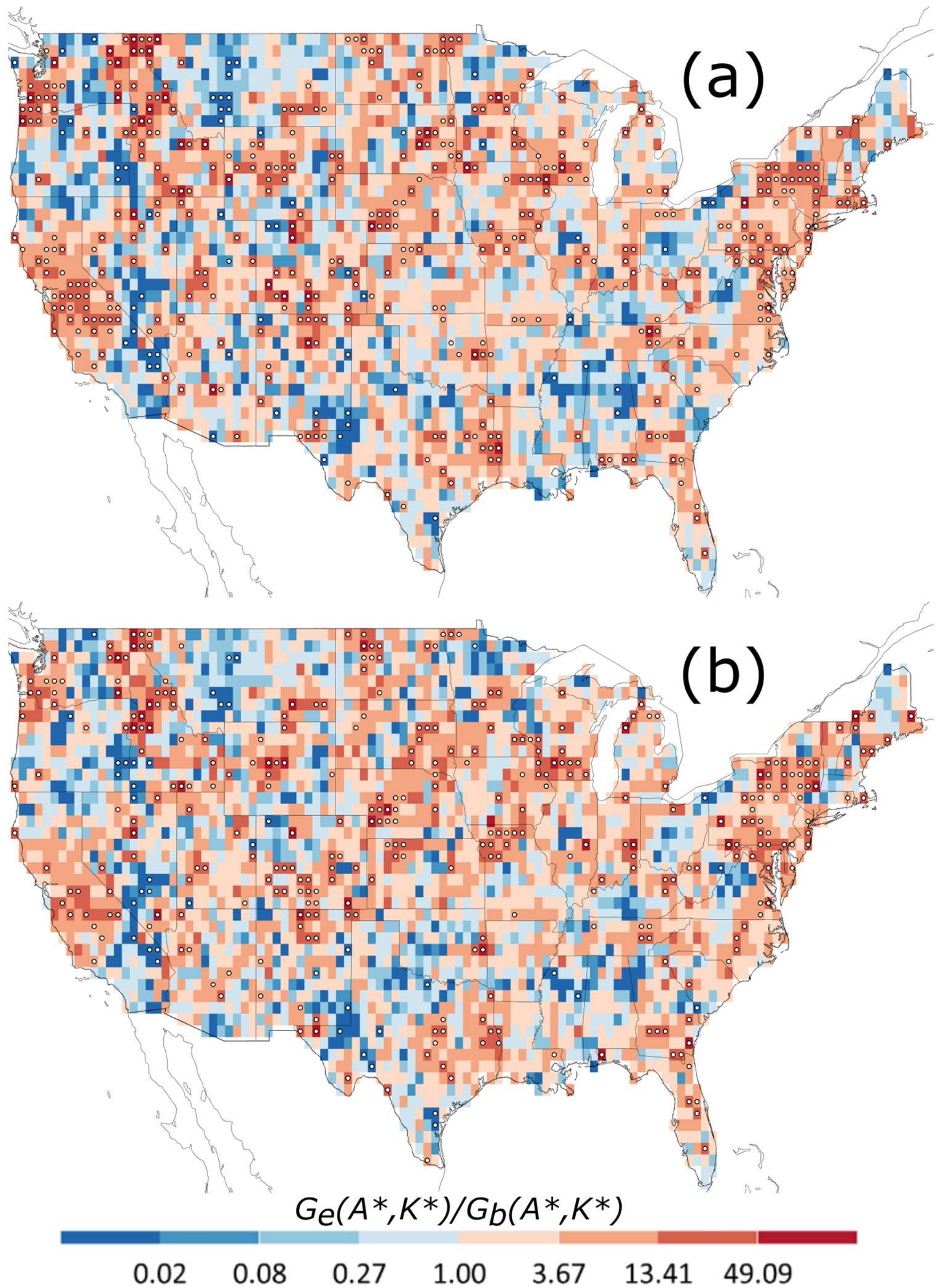

Figure 3. Spatial trends in the probability of joint exceedances of A and K, i.e., joint occurrence of annual maximum daily precipitation event exceeding its 100-year return level following a k-day precedent precipitation total greater than its 10-year return level, for (a) k=5 and (b) k=30. Statistically significant estimates (p-value < 0.05) are represented with white circles. The color indicates the ratio of the probability at the end of the given period to the probability at the beginning. Details of the ratio are presented in Equation (11).